

Completing the puzzle of the 2004–2005 outburst in V 0332+53: the brightening phase included

S. S. Tsygankov^{1,2*}, A. A. Lutovinov², and A. V. Serber³

¹*MPI for Astrophysics, Karl-Schwarzschild str. 1, Garching, 85741, Germany*

²*Space Research Institute of the Russian Academy of Sciences, Profsoyuznaya str. 84/32, Moscow 117997, Russia*

³*Institute of Applied Physics of the Russian Academy of Sciences, 46 Ulyanov st., 603950 Nizhny Novgorod, Russia*

Accepted Received ...

ABSTRACT

Analysis of the data obtained with the RXTE observatory during a powerful outburst of the X-ray pulsar V 0332+53 in 2004–2005 is presented. Observational data covering the outburst brightening phase are analysed in detail for the first time. A comparison of source parameters and their evolution during the brightening and fading phases shows no evidence for any hysteresis behaviour. It is found that the dependences of the energy of the cyclotron absorption line on the luminosity during the brightening and fading phases are almost identical. The complete data sequence including the outburst brightening and fading phases makes it possible to impose the more stringent constraints on the magnetic field in the source. The pulse profile and pulsed fraction are studied as functions of the luminosity and photon energy.

Key words: X-ray:binaries – (stars:)pulsars:individual – V 0332+53

1 INTRODUCTION

It is conventionally believed that the structure of accretion environment of a strongly magnetized neutron star in an X-ray pulsar, as well as its emission, are actually governed by a few key parameters such as the neutron-star spin period and magnetic field, the binary orbital period and separation of the companions, and of course the accretion rate \dot{M} . Sporadic outbursts occurring in some X-ray pulsars when the bolometric X-ray luminosity L_X increases due to an enhanced accretion rate provide for the possibility of probing the observable response of such a complex system as an accreting X-ray pulsar to varying \dot{M} and getting more insight into the accretion onto a strongly magnetized neutron star and the accompanying high-energy emission.

In particular, it is known since GINGA observations of the X-ray pulsar 4U 0115+63 in 1990–1991 (Mihara et al. 1998) that the energies of cyclotron absorption features observed in X-ray pulsar spectra can vary with their luminosities. Such variations are conventionally interpreted in terms of the luminosity dependence of the height of the line-forming region above the neutron-star surface (Basko & Sunyaev 1976). The correspondent negative correlation between the cyclotron-line energy and the luminosity was observed to date for several bright X-ray pulsars (e.g. Mihara et al. (1998); Tsygankov et al. (2006)). Note

that the opposite case of the positive correlation was also registered at least for one or two X-ray pulsars (e.g. see Staubert et al. (2007) for Her X-1 and La Barbera et al. (2005); Filippova et al. (2005) for GX301-2).

It should be emphasized that, to date, cyclotron-line parameters for all sources were mostly studied during fading phases of outbursts because of time lags between the beginning of an outburst and the start of observations. For example, it was shown by Tsygankov et al. (2006) (hereafter referred to as Paper I) that the energy of the cyclotron line observed in spectra of the X-ray pulsar V 0332+53 increases almost linearly with decreasing luminosity during the fading phase of an outburst in 2004–2005.

This paper presents a comprehensive analysis of temporal and spectral parameters of V 0332+53 over a nearly complete powerful outburst of 2004–2005, including the brightening phase studied in detail for the first time.

2 OBSERVATIONS AND DATA ANALYSIS

This work employs the RXTE data (Bradt et al. 1993) acquired during the observations with the following IDs: 90014-XX-XX-XX, 90089-XX-XX-XX and 90427-XX-XX-XX. Note that Paper I was based only on the ID 90427-XX-XX-XX data covering the fading phase of the outburst. Since the aims of the present work and Paper I are slightly different, these data were reanalyzed to ensure the unifor-

* E-mail: sst@mpa-garching.mpg.de

mity with the IDs 90089-XX-XX-XX and 90014-XX-XX-XX corresponding to the brightening and fading phases of the outburst, respectively.

In general, the data-analysis procedure was identical to that used in Paper I. The luminosity was calculated assuming a source distance of 7 kpc (Negueruela et al. 1999). Note that the correct account of the dead time is crucial since the source count rate reached very high values. Using improved software, we recalculated the luminosities for the observations in the ID 90427 set and found that the luminosities for a few brightest epochs of this set are to be lowered by about 15–20% in comparison with the values published in Paper I. Note, these corrections are not too large to affect the conclusions of Paper I. The time dependence of the bolometric luminosity in the photon energy range 3–100 keV during the outburst of 2004–2005 is shown in Fig. 1. All the data are naturally grouped into the brightening (filled green squares) and fading phases (open blue circles) of the outburst. For comparison, the result of INTEGRAL observations are also plotted by the triangles in this figure (see Paper I). The solid line is the rescaled light curve obtained with the ASM monitor in the photon energy range 2–12 keV. Further data reduction for both PCA and HEXTE spectrometers was done using standard tools of FTOOLS/LHEASOFT 6.3.2 package.

Since the source was bright and the outburst was nearly completely covered with the RXTE observations (see Fig. 1), it is possible to obtain the high-quality broadband energy spectra of the source at different stages of the outburst and study the evolution of source parameters with the luminosity and the outburst phase. It was noted in Paper I that the best-fit cutoff energy $E_{\text{cut}} \simeq 5-6$ keV for the XSPEC *powerlaw*×*highcut* model (White et al. 1983), which is usually used for approximation of X-ray pulsars spectra, is close to the lower limit (~ 3 keV) of the PCA energy range, so that the photon index cannot be accurately retrieved from such a continuum model. Hence, the continuum spectrum of the source was fitted with the simpler *cutoffpl* model which describes the source spectrum similarly well, but has fewer parameters and is free of the above limitations. The continuum spectrum was modified by one or few cyclotron-harmonic line features depending on the source luminosity. A cyclotron absorption line was fitted with the Lorentz profile (Mihara et al. 1990)

$$\exp\left(\frac{-\tau_{\text{cycl}}(E/E_{\text{cycl}})^2\sigma_{\text{cycl}}^2}{(E-E_{\text{cycl}})^2+\sigma_{\text{cycl}}^2}\right),$$

where E_{cycl} , σ_{cycl} , and τ_{cycl} are the line central energy, width, and depth, respectively. The fundamental cyclotron line (below we'll call it "the cyclotron line" for a simplicity) is clearly detected in all observations, whereas the second-harmonic line was confidently observed not in all data sets. In some cases, inclusion of the third harmonic in the model affected the parameters of the second-harmonic line. The third harmonic itself was registered and its parameters can be more or less reliably retrieved only for several brightest states (see Paper I for details). We examined possible effects of including the second harmonic in the fit on the parameters of the cyclotron line and the continuum. In these tests, the central energy of the second-harmonic line was either a free parameter or fixed equal to two times the central energy of the cyclotron line. It was found that the cyclotron

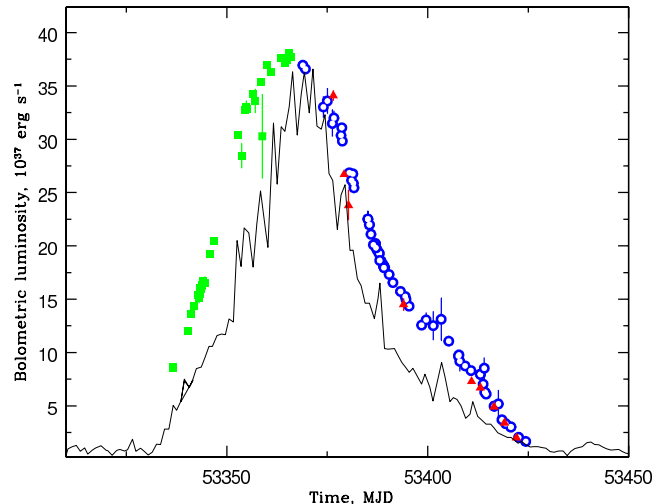


Figure 1. Temporal dependence of the V 0332+53 luminosity during the outburst of 2004–2005. Filled green squares and open blue circles correspond to the brightening and fading phases, respectively. The triangles are INTEGRAL results. The solid line is the rescaled ASM light curve. The error bars here and in the entire paper correspond to $\pm 1\sigma$.

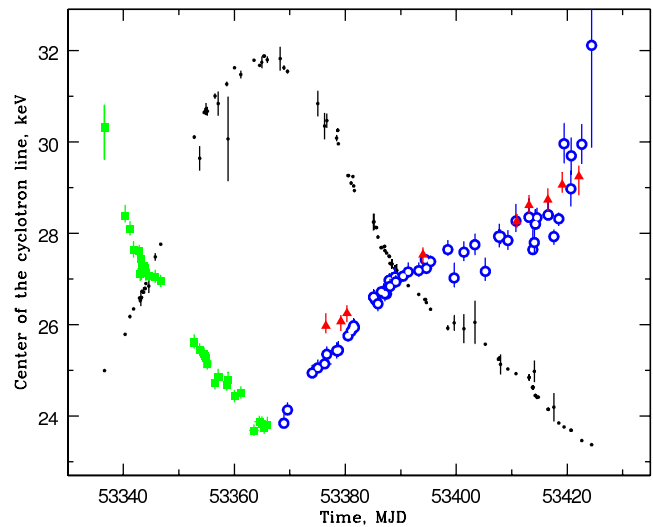


Figure 2. Temporal evolution of the cyclotron-line energy during the V 0332+53 outburst. The source bolometric luminosity is shown with the small black circles. Other symbols are the same as in Fig.1.

line and continuum parameters do not depend within errors on the higher harmonics.

3 RESULTS

This section presents the results of spectral analysis during almost entire outburst of V 0332+53. The analysis is focused on the source spectral parameters as functions of the luminosity and time.

V 0332+53 is one of two X-ray pulsars whose spectra exhibit at least three cyclotron-harmonic absorption line features (Coburn et al. 2005; Kreykenbohm et al. 2005). In

general, this source has a fairly complex, multi-component spectrum. Therefore, we applied the above-described spectral model including a power law with an exponential cutoff, up to three absorption lines depending on the source brightness and "detectability," and the 6.4-keV iron emission line which was clearly observed in all states of the source. Since the iron line was narrow and the energy resolution of the PCA spectrometer at 6–7 keV was limited ($\sim 18\%$), the actual line width cannot be accurately determined. Thus, a fixed value of 0.1 keV was used in the XSPEC data analysis.

Variations in the main spectral parameters with the time and the luminosity are described in detail below.

3.1 Cyclotron Energy Versus Luminosity

It was mentioned above that variations in the cyclotron-line energy and their possible dependence on the luminosity were discovered and reported by Mihara et al. (1998) for several bright X-ray pulsars. The cyclotron-line energy – source luminosity relation was studied in detail for the first time by Tsygankov et al. (2006) for V0332+53 in a wide luminosity range. Using INTEGRAL and RXTE data obtained during the fading phase of the 2004–2005 outburst, they discovered the strong negative correlation between the cyclotron line energy and the luminosity which can be described fairly well by a linear function.

Including both the fading and brightening phases of the outburst into an analysis makes it possible to study the possible difference in the cyclotron-line behavior during these outburst stages to verify the hypothesis on the hysteretic dependence of the source parameters on its luminosity. Figure 2 shows the temporal evolution of the cyclotron-line energy during the entire outburst. Distinct asymmetry of this time profile can obviously be attributed to the asymmetry of the outburst light curve. The existence of hysteresis the cyclotron-line energy as a function of the source was checked by constructing this dependence for the entire outburst (see Fig. 3). The resulting plot unambiguously rules out the hysteresis hypothesis. This is valid for luminosity above $\sim 1.5 \times 10^{38}$ erg s $^{-1}$ (the lower-luminosity data are absent in the brightening phase). Hence, the physics of accretion column and its emission is essentially same at both these stages.

A formal linear fit of this dependence (all available measurements have been used), $E_{\text{cycl},1}[\text{keV}] \simeq -0.143(\pm 0.002)L_{37} + 29.56(\pm 0.03)$ (here, L_{37} is the luminosity in the units of 10^{37} erg s $^{-1}$, uncertainties correspond to a 90% confidence level), is practically the same as the one obtained in Paper I for only the fading phase of the outburst and even takes into account the above-mentioned luminosity corrections for several highest-count-rate observations. Note, however, that allowance for these corrections makes the behavior of the cyclotron energy at very high luminosities $> 3.5 \times 10^{38}$ erg s $^{-1}$ slightly different from this fit: the "rate" of the cyclotron-energy variations is higher. Such a difference (if any) may be connected with possible changes in the accretion-flow structure and emission at very high luminosities then the source can transfer into other accretion regime. On the other hand, poor statistics impedes finalizing conclusions on the behavior of the cyclotron-line energy at low luminosities below $L_{37} \simeq 5$. Some evidence is seen in Fig. 3 for "steepening" of the cyclotron energy – luminosity slope below $\simeq 4 \times 10^{37}$ erg s $^{-1}$, but its significance is not

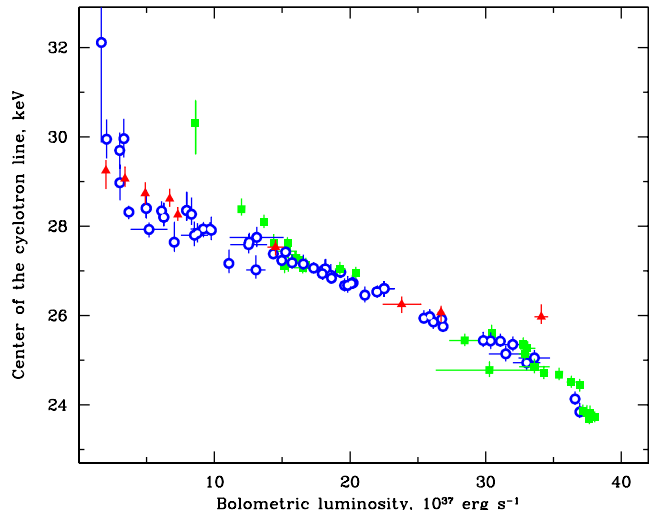


Figure 3. The cyclotron-line energy versus the luminosity L_{37} . Symbols are the same as in Fig.1.

enough for the final conclusion. Note, that the behavior of the cyclotron energy at low luminosities is very interesting from the viewpoint of determining the so-called critical luminosity at which the shock wave at the top of the accretion column disappears and/or detecting the same reverse dependence (if any) of the cyclotron-line energy with the luminosity as was observed for Her X-1 (Staubert et al. 2007).

Meanwhile, the lowest observed value of the cyclotron energy in the V0332+53 spectrum provides for an estimate for the magnetic field on the neutron-star surface. Unfortunately, the lowest-luminosity data point in Fig.3 has fairly large uncertainty. Hence, it seems more expedient to use the result from the linear fit, that is 29.56 keV. This yields

$$B_{\text{NS}} = (1 + z) \times \frac{29.56}{11.6} \simeq 3.1 \times 10^{12} \text{ G},$$

where z is the gravitational redshift near the surface of a neutron star with a radius of 10 km and a mass of $1.4M_{\odot}$.

3.2 Equivalent Width of the Cyclotron Line

It is well known from the classical stellar spectral analysis that the equivalent width of a spectral line is a very important quantity for retrieving physical parameters and conditions in the line-forming region. Hence, in addition to such cyclotron-line model parameters as σ_{cycl} and τ_{cycl} , it seems expedient to have an observable quantity playing the role of cyclotron-line equivalent width in X-ray astrophysics and quantifying the total number of photons withdrawn from the continuum spectrum of a source due to resonance scattering in the cyclotron line(s). The main problem in calculating the cyclotron-line equivalent width is its strong dependence on the adopted continuum model to be multiplied by the line models typically used to fit cyclotron-harmonic lines. We used the following simple technique to calculate the cyclotron-line equivalent width EW_{cycl} : (1) All energy channels affected by the cyclotron line (typically 18–40 keV) are excluded from the source spectrum; (2) The remaining energy bins are fitted as a spectrum of the continuum; (3) The energy bins excluded at step 1 are added again to the spectrum, their deviations from the continuum fit obtained at

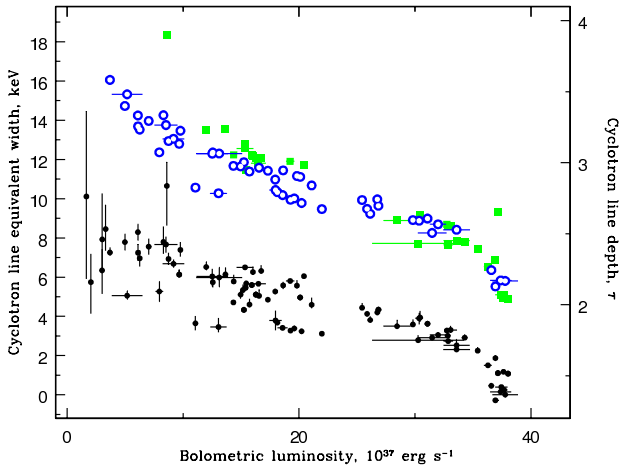


Figure 4. Dependence of the equivalent width EW_{cycl} (open circles and filled squares) and the depth τ_{cycl} (filled circles) of the cyclotron line in V0332+53 spectra on the pulsar luminosity L_{37} . Symbols are the same as in Fig.1.

step 2 is calculated, and, upon normalization to the continuum spectrum, are integrated over energy; (4) The resulting energy-integrated deviation of the normalized cyclotron-line energy bins from the continuum fit is adopted as a measure for the equivalent width EW_{cycl} of the cyclotron line¹.

It was found that the quantity EW_{cycl} calculated in such a way is not constant, but varies with the cyclotron-line energy changes during the outburst. The EW_{cycl} dependence on the luminosity is shown in Fig. 4. As in Fig. 3, different symbols such as filled squares and open circles correspond to the brightening and fading phases of the outburst, respectively. The cyclotron-line equivalent width decreases almost linearly with the luminosity repeating the behavior of the cyclotron-line energy itself, including the increase of the "rate" of the equivalent width changes at high luminosities. But it is necessary to note, that the slope of this formal linear relation $EW_{\text{cycl}}[\text{keV}] \propto -0.25L_{37}$ is different from that in Fig.3. It is also worthy to note the similar behaviour of the cyclotron line optical depth τ_{cycl} (see filled circles in Fig. 4), that can be understood from the revealed linear correlation between τ_{cycl} and EW_{cycl} .

The correlation between the cyclotron-line energy E_{cycl} and its width σ_{cycl} has been noted earlier in several works (Heindl et al. 1999; Dal Fiume et al. 2000; Coburn et al. 2002; Staubert 2003) for a number of X-ray pulsars with different cyclotron line energies and viewing angles. The last one can play an important diagnostic role. In particular, it was used by Staubert (2003) to explain nondetection of cyclotron lines in certain objects.

Note, that the relation between σ_{cycl} and E_{cycl} stems

¹ We should note, that the spectrum of V0332+53 contains a few harmonics of the cyclotron line and it is practically impossible to avoid fully the influence of absorption features to the continuum component. Therefore, obtained values of the equivalent width should be treated only for the demonstration of the qualitative behaviour. Such an analysis was carried out for sufficiently bright observations.

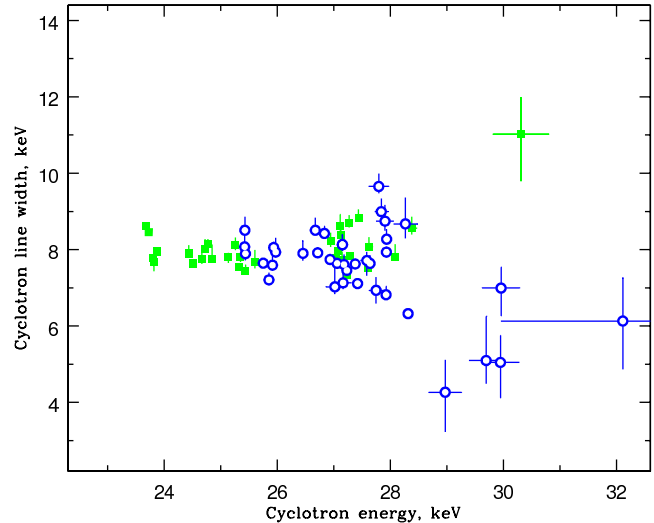


Figure 5. Cyclotron-line width σ_{cycl} versus cyclotron energy E_{cycl} for all observed luminosities. Symbols are the same as in Fig.1.

from both the Doppler broadening due to thermal motion of electrons along the magnetic field in the line-forming region and the natural cyclotron-line broadening giving rise to broad Lorentz-shaped wings of the line. The observed Doppler width of the cyclotron line is (Trümper et al. 1977; Meszaros 1992)

$$\sigma_{\text{cycl,D}}^{\text{obs}} = E_{\text{cycl}}(2\kappa T_e/mc^2)^{1/2} \langle \cos \alpha_{\text{obs}} \rangle,$$

where $\langle \dots \rangle$ denotes averaging over the duration of one observation which is typically about a few kiloseconds, i.e., much longer than the X-ray pulsar period,

$$\alpha_{\text{obs}} = \arccos[\cos \Theta_{\text{obs}} \cos \Theta_* + \sin \Theta_{\text{obs}} \sin \Theta_* \cos \Phi_*(t)]$$

is the angle between the magnetic field in the line-forming region and the observer line of sight, Θ_{obs} is the angle between the neutron-star spin axis and the line of sight, Θ_* is the angle between the neutron-star spin and magnetic axes, Φ_* is the angle between the neutron-star magnetic axis and the plane comprising the neutron-star spin axis and the line of sight, and T_e is the electron temperature. In the absence of neutron-star precession effects, $\Theta_{\text{obs}} = \text{const}$ over the binary orbit. Hence, $\langle \cos \alpha_{\text{obs}} \rangle = \cos \Theta_{\text{obs}} \cos \Theta_* = \text{const}$ and $\sigma_{\text{cycl,D}}^{\text{obs}}/E_{\text{cycl}} = (2\kappa T_e/mc^2)^{1/2} \cos \Theta_{\text{obs}} \cos \Theta_*$. Note, however, that the applied fit of the cyclotron line implies that the natural broadening implying the Lorentz profile of the cyclotron line is assumed dominant. In this case, the observed relative cyclotron-line width $\sigma_{\text{cycl,L}}^{\text{obs}}/E_{\text{cycl}} = (4e^2/3\hbar c)(E_{\text{cycl}}/mc^2) \propto E_{\text{cycl}}$ is independent of the system geometry and the electron temperature in the source. In addition, the ratio $\sigma_{\text{cycl}}/E_{\text{cycl}}$ can also be contributed by other factors, e.g., nonuniformity of the magnetic field over the line-forming region.

We examined the processed data for the presence of linear correlation between σ_{cycl} and E_{cycl} . The cyclotron line width as a function of its energy for V0332+53 during its 2004–2005 outburst is shown in Fig. 5. No pronounced linear increase in σ_{cycl} with increasing E_{cycl} is seen. The typical width of the cyclotron line is about 8 keV. The fairly strong scatter of the data points for large cyclotron energies

is probably caused by spectrum-statistics worsening at the low luminosities. This is confirmed indirectly by an increase in the error-bar sizes. An additional factor which affect to the observable broadening of the cyclotron line can be the finite energy resolution of the HEXTE spectrometer (FWHM is about 5.5 keV at 30 keV).

Finally note that according to the theory of cyclotron-radiation transfer under neutron-star conditions (see, e.g., (Zheleznyakov & Serber 1993)), the optical depth at the cyclotron line varies only slightly with α_{obs} and can hardly exclude the formation of a resonance scattering feature at fairly large α_{obs} . Hence, the cyclotron line nondetection should rather be related to specific viewing conditions of the line-forming region such as its small visible area or screening of this region by the neutron star and/or accretion disc/stream.

3.3 Pulse-Profile Variations

It is well known that pulse profiles of X-ray pulsars are strongly dependent on the photon energy and luminosity. This is especially prominent in soft energy bands strongly affected by the intrinsic absorption in the binary. As the photon energy increases toward the hard X-ray range, the observed emission becomes progressively less sensitive to the poorly known environment of the accreting neutron star and carries more and more imprints of actual physical and geometrical parameters in hot polar-cap regions on the neutron star where this radiation is generated. Although these regions are believed to be much simpler in structure and physics, strong changes of pulse profiles are observed in their hard X-ray emission, as well. In particular, this was demonstrated by Lutovinov & Tsygankov (2009) who used INTEGRAL data to reconstruct uniformly the pulse profiles of ten bright X-ray pulsars in hard X-rays for different luminosities and study their variability.

This section is aimed at answering the question on the absence or presence of pulse-profile hysteretic behavior during the brightening and fading phases of the outburst from V 0332+53. It was shown in the previous sections that the source spectrum and its parameters are practically the same at the outburst stages with the same luminosity. Taking into account the similarity of pulse profiles at the same luminosities for the brightening and fading phases of an outburst from 4U 0115+63 (Tsygankov et al. 2007) we can expect the similar behavior for V 0332+53.

According to Paper I, the main mystery of the considered source is the drastic change of its pulse profile near the cyclotron line. In particular, it was shown that the pulse profile in the high-luminosity state ($L_{37} \sim 35$) has a sinusoidal double-peaked shape at all energies. The relative intensities of the pulses are slightly different. Very small variations in the positions of the peaks depending on the photon energy range were observed. As the pulsar luminosity decreases, the pulse profile changes significantly. In the soft energy bands (at photon energies less than $\simeq 8$ keV) it becomes nearly single-peaked. One the intra-peak gap disappears and the double-peaked profile transforms into an asymmetrical single-peaked one at energies near the cyclotron line. Then the pulse profile becomes double-peaked again with the further increase in the photon energy.

Here, all the data covering the outburst of 2004–2005, including the ID 90427 used in Paper I, are reanalyzed

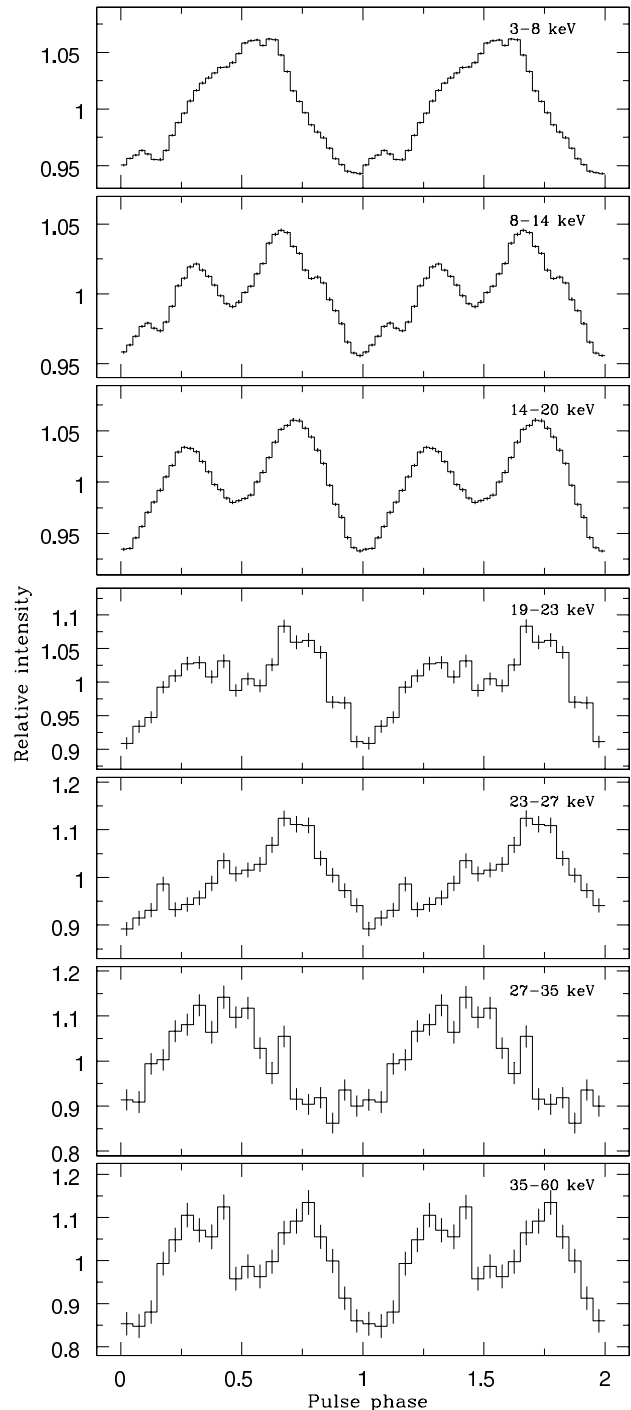


Figure 6. Pulse profiles of V 0332+53 for the RXTE observation 90089-11-02-03 during the brightening phase of the 2004–2005 outburst for the luminosity $L_{37} \simeq 16$ and the cyclotron-line energy $E_{\text{cycl}} \simeq 27.2$ keV

uniformly and a detailed comparison of pulse profiles corresponding to the same luminosities during the outburst brightening and fading phases is made. It is found that they are similar to each other (minor differences may only exist in the softest energy band < 8 keV) and their behavior with the luminosity identical to the described above. Note, that for several highest-luminosity observations it was impossi-

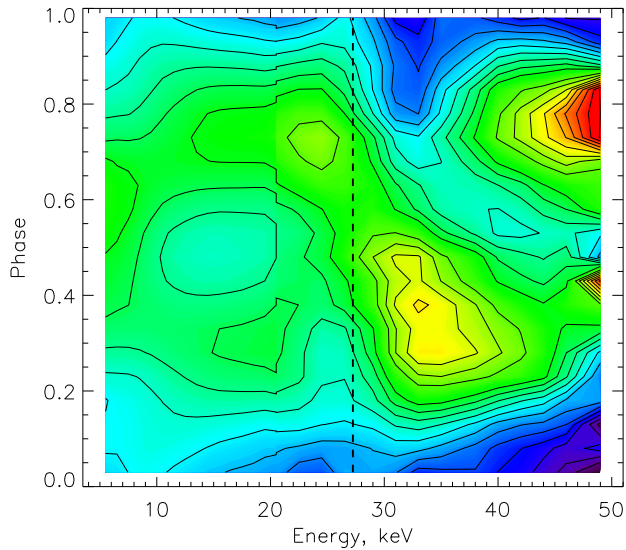


Figure 7. Two-dimensional distribution of V0332+53 pulse-profile intensities (normalized to unity) over the photon energy and the pulse phase for the RXTE observation 90089-11-02-03 during the brightening phase of the 2004–2005 outburst for the luminosity $L_{37} \simeq 16$. Position of the cyclotron line center is shown by the dashed line. Red colour corresponds to higher and blue to lower relative intensities. Solid lines represent levels of equal intensity: 0.20, 0.24, 0.28, ..., 0.96, 1.00.

ble to produce the pulse profiles using PCA data due to the absence of data modes with sufficient energy and time resolution below 20 keV.

For illustrative purposes the pulse profiles in different energy bands for the observation 90089-11-02-03 (the luminosity was 1.6×10^{38} erg s $^{-1}$ at the brightening phase) are shown in Fig.6. The PCA channels correspond to 3–8, 8–14 and 14–20 keV to demonstrate changes at soft photon energies and the transition from single- to double-peak shape. Following Paper I, the hard energy channels (HEXTE data) were chosen to divide the cyclotron line in equal parts.

It is seen that relatively far from the cyclotron energy equal to $\simeq 27.2$ keV for this observation, the pulse profile is double-peaked with a domination of a second peak in the photon energy range 19–23 keV. In the left (“soft”) wing of the cyclotron line the profile is become single-peaked with its center at the pulse phase of ~ 0.65 . In the right (“hard”) wing of the cyclotron line the profile is also single-peaked, but the position of its maximum is shifted to the pulse phase ~ 0.3 . At the higher energies the pulse profile becomes double-peaked again. Note, that the observed shifting of the peak over the phase near the cyclotron line energy is occurred gradually with increasing photon energy. These features can be seen clearly in Fig.7 plotted using the technique described in detail in Paper I.

Note that the observed pulse profile is contributed by three main components: (i) direct radiation coming from one or two under-the-shock hot polar columns which produce(s) the continuum and hosts the cyclotron-line-forming region being presumably the upper part of the column adjacent to the shock, (ii) forward-scattered radiation outgoing from the side of the accretion stream feeding the “front” (directly visible) polar column and (iii) backward-scattered

radiation outgoing from the side of the accretion stream feeding the “back” (neutron-star shaded) polar column. Quantitative pulse-profile modeling is a complicated problem requiring good knowledge of the features of radiation beaming near the cyclotron frequency (Gnedin & Sunyaev 1973; Pavlov et al. 1985). In particular, it was shown by Meszaros & Nagel (1985) that the accretion column beam function at the cyclotron energy is significantly different from the radiation beaming at other energies.

3.4 Pulsed Fraction Dependence on the Energy and Luminosity

It was already observed that the pulsed fraction $PF = (I_{\max} - I_{\min}) / (I_{\max} + I_{\min})$, where I_{\max} and I_{\min} are maximum and minimum intensities in the pulse profile of an X-ray pulsar, respectively, increases with energy in the hard X-rays (> 20 keV) for all studied sources (see e.g. Staubert et al. (1980); Frontera et al. (1985) and a last review of Lutovinov & Tsygankov (2009) and references therein). However, this increase is not monotonic for some sources and shows such local features as, e.g., maxima near the cyclotron lines. The pulsed fraction as a function of the photon energy was studied in detail in a wide energy band (3–100 keV) for the pulsar 4U 0115+63 using the RXTE data (Tsygankov et al. 2007). It was found in this paper that (i) the pulsed fraction increases with the photon energy and decreased with the luminosity and (ii) the local PF maxima (hump-like features) exist not only near the cyclotron line, but also near the higher harmonics. Note that Ferrigno et al. (2009) analyzed archival BeppoSAX data for 4U0115+63 and found a local decrease in the pulsed fraction near the second cyclotron harmonic in the middle of the fading phase.

In this work, the V 0332+53 pulsed fraction is analyzed in various photon energy ranges and for different luminosity states using the same complex approach that was employed by Tsygankov et al. (2007) for 4U 0115+63.

Figure 8 shows the energy dependences of the pulsed fraction for observations with various pulsar luminosities obtained in a wide photon-energy range for the brightening and fading phases of the outburst. The corresponding luminosities in the units of 10^{37} erg s $^{-1}$ are indicated to the right of each plot. It is seen that the behavior of the V 0332+53 pulsed fraction at high energies (> 20 keV) is typical of X-ray pulsars (see, e.g., Lutovinov & Tsygankov (2009)). In particular, the pulsed fraction increases with the photon energy and the form of the increasing function $PF(E)$ depends on the luminosity, but changes only slightly over a wide luminosity range and is roughly the same for similar luminosities during the brightening and fading phases of the outburst.

On the contrary, these dependencies for soft energy bands are very different. We should specially note the photon energies below 12–15 keV for which an increase in the pulsed fraction with decreasing photon energy is observed for the first time. Such behavior observed in a wide luminosity range is the most prominent for luminosities $< 1.5 \times 10^{38}$ erg s $^{-1}$. It is difficult to explain it within the framework of known models since, in particular, no significant absorption was observed in the source spectrum during the entire outburst. Further detailed studies are required to clarify this problem and we plan to perform such an analysis in a separate paper.

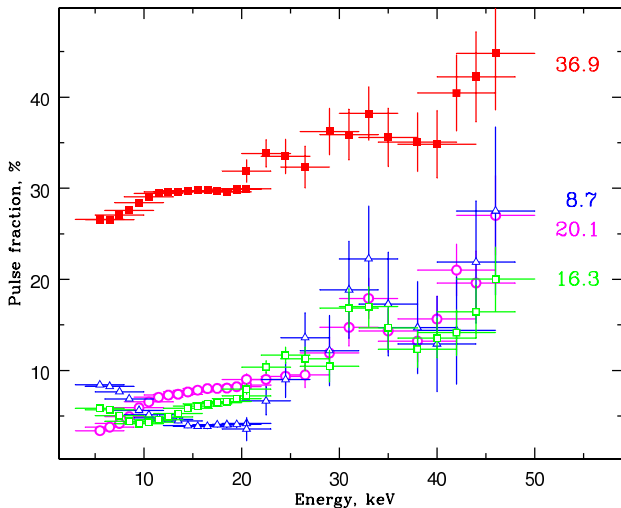


Figure 8. Energy dependences of V 0332+53 pulsed fraction during the brightening and fading phases of the outburst. Different symbols correspond to different source luminosities indicated to the right of each plot in the units of 10^{37} erg s^{-1} . The green open and red filled squares correspond to $L_{37} \simeq 16.3$ and $L_{37} \simeq 36.9$, respectively, during the brightening phase (RXTE observations 90089-11-02-03 and 90089-11-04-04, respectively). The magenta open circles and blue open triangles correspond to $L_{37} \simeq 20.1$ and $L_{37} \simeq 8.7$, respectively, during the fading phase (RXTE observations 90014-01-02-00 and 90014-01-05-02, respectively).

Here, we only note a steep rise in the pulsed fraction from $\sim 10\%$ to $\sim 30\%$ with an increase in the luminosity from $\sim 2 \times 10^{38}$ to $\sim 3.5 \times 10^{38}$ erg s^{-1} and changes in the pulsed fraction behavior in the soft energy bands.

It should also be noted that the V 0332+53 pulsed fraction at soft energies is small in comparison with values observed for other X-ray pulsars. This fact was mentioned previously by Mihara et al. (2007) who attempted to explain this feature assuming that the angles Θ_{obs} and/or Θ_* are small. However, both these assumptions can hardly be conformed with the observed high values of the high-energy and high-luminosity pulsed fraction and the observed energy and luminosity dependence of the pulsed fraction.

The most interesting feature at the high energies is a local pulsed fraction maximum near the cyclotron-line energy. Such a hump-like feature is observed for almost any luminosity during both brightening and fading phases of the outburst. To rule out its possible artefact origin caused either by the HEXTE data itself, we obtained the pulsed fraction dependence on the energy using the INTEGRAL data (Lutovinov & Tsygankov (2009), see also <http://hea.iki.rssi.ru/integral/pulsars/index.php>). Figure 9 shows how the pulsed fraction changes with the energy for two values of the luminosity. The RXTE/HEXTE and INTEGRAL/ISGRI results are shown by the open circles and filled triangles, respectively. The upper and lower panel of the figure correspond to the high and low luminosities $L_{37} \sim 25$ and $L_{37} \sim 5$, respectively. It is clearly seen for both luminosities that the pulsed fraction dependencies are practically the same for the RXTE and INTEGRAL data

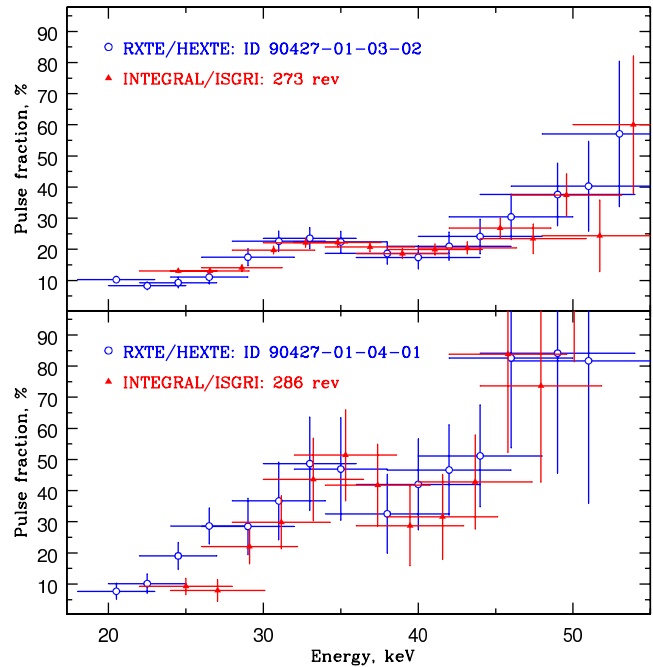


Figure 9. Energy dependences of the V 0332+53 pulsed fraction during the high- (upper panel) and low-luminosity states (bottom panel). The filled triangles represent INTEGRAL/ISGRI data during revolutions 273 (high state) and 286 (low state). The open circles are RXTE/HEXTE data during observations 90427-01-03-02 (high state) and 90427-01-04-01 (low state).

and the ”hump”-like features are clearly detected in both data sets. We analyzed all the available HEXTE data and found that the ”hump” energy ($E_{\text{hump}} \simeq 32\text{--}34$ keV) is more or less stable over a wide luminosity range. This can imply that such a pulsed fraction ”hump” is possibly related to some intrinsic properties of the neutron-star magnetosphere rather than to the local cyclotron energy corresponding to the current luminosity. Finally, it is interesting to note that the energy of this ”hump”-like feature is about of the maximum measured value of the cyclotron energy for this source (see Section 3.1) corresponding to the magnetic field at the surface of the neutron star.

It was shown by (Lutovinov & Tsygankov 2008, 2009) that the pulsed fraction in a wide energy band usually decreases with increasing luminosity of an X-ray pulsar. This fact was preliminarily explained within the framework of a geometrical model in which the pulsed fraction is determined by the luminosity-dependent visible areas of the accretion columns.

The luminosity dependence of the pulsed fraction in the photon energy range 25–45 keV is shown in Fig. 10. The observed behavior does not fully conform to the predictions of the above-mentioned model. Whereas the pulsed fraction decreases with increasing luminosity below $\sim 10^{38}$ erg s^{-1} in accordance with this model, its value remains almost constant at a level of $\sim 10\%$ in the luminosity range $(1\text{--}2) \times 10^{38}$ erg s^{-1} and rises almost linearly at higher luminosities. Note that the luminosity dependence of the pulsed fraction is the same for both brightening and fading phases of the outburst.

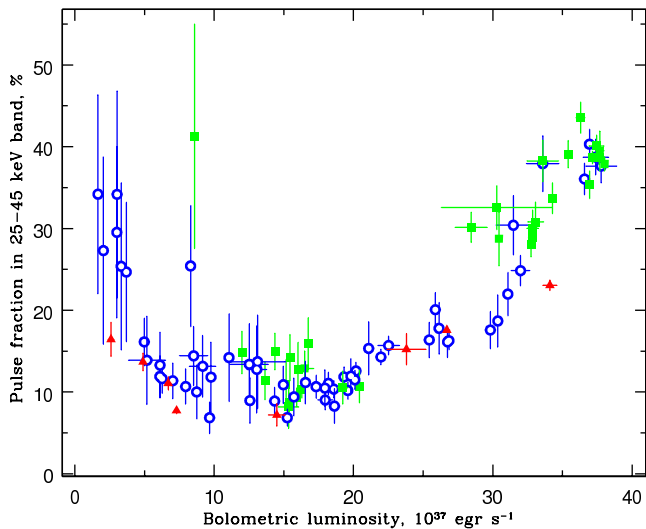


Figure 10. Pulsed fraction in the photon energy range 25 – 45 keV versus the V 0332+53 bolometric luminosity. As before, squares, circles and triangles of different types represent the RXTE/HEXTE data covering the brightening and fading phases of the outburst at rising and decay parts of the outburst and the INTEGRAL/ISGRI data, respectively.

4 SUMMARY

The main results of the present work can be summarized as follows:

1. The brightening phase of the 2004–2005 outburst in the X-ray pulsar V 0332+53 is studied in detail for the first time, thereby completing an analysis of the evolution of the accreting X-ray pulsar parameters over an entire outburst.

2. It is shown that the equivalent width EW_{cycl} demonstrates the strong positive linear correlation with the cyclotron-line depth τ_{cycl} and, similar the cyclotron-line energy E_{cycl} , decreases almost linearly with the bolometric luminosity L_X .

3. The hypothesis of hysteretic behavior of the observed radiation during the brightening and fading phases of the outburst was checked and can be ruled out. In particular, the source spectrum and its parameters and the pulsed fraction behavior are practically the same at the outburst stages with the same luminosity.

4. The presence of a local hump-like feature near the cyclotron-line energy in the pulsed fraction as a function of the photon energy is confirmed. Its position remains nearly constant at about $E_{\text{cycl,max}}$.

5. An increase in the pulsed fraction with decreasing photon energy below 12 – 15 keV is observed for the first time in several observations.

6. The dependence of the pulsed fraction in the energy range 25–45 keV on the V 0332+53 bolometric luminosity during the brightening phase of the 2004–2005 outburst is found and compared with the similar dependence for the fading phase of the same outburst. No hysteretic behavior is observed. It was revealed for the first time that the pulse fraction rises almost linearly at higher luminosities.

ACKNOWLEDGMENTS

We thank the referee for his useful comments and suggestions. This work was supported by the Russian Foundation for Basic Research (project no.07-02-01051 and 08-08-13734), the Program “Origin, Structure and Evolution of the objects in the Universe” (P07) by the Presidium of the Russian Academy of Sciences and grant no.NSh-5579.2008.2 from the President of Russia. We are grateful for the data to the High Energy Astrophysics Science Archive Research Center Online Service provided by the NASA/Goddard Space Flight Center.

REFERENCES

- Basko M.M., Sunyaev R.A., 1976, MNRAS, 175, 395
 Bradt H.V., Rothschild R.E., Swank J.H., 1993, A&AS, 97, 355
 Coburn W., Heindl W., Rothschild R., et al., 2002, ApJ 580, 394
 Coburn W., Kretschman P., Kreykenbohm I., et al., 2005, Astron. Telegram, 381, 1
 Dal Fiume D., Orlandini M., Sordo S., et al., 2000, AdSpR, 25, 399
 Frontera F., Dal Fiume D., Morelli E., Spada G., 1985, ApJ, 298, 585
 Ferrigno C., Becker P., Segreto A., et al., 2009, A&A, 498, 825
 Filippova C., Tsygankov S., Lutovinov A., Sunyaev R., 2005, Astron. Lett., 31, 729
 Gnedin Yu., Sunyaev R., 1973, A&A, 25, 233
 Heindl et al. 1999, ApJ 521, L49
 Kreykenbohm I., Mowlavi N., Produit N., et al., 2005, A&A, 433, L45
 La Barbera A., Segreto A., Santangelo A., et al., 2005, A&A, 438, 617
 Lutovinov A.A., Tsygankov S.S., 2008, AIP Conference Proceedings, 1054, 191
 Lutovinov A.A., Tsygankov S.S., 2009, Astron. Lett., 35, 433
 Lyubarskii Yu., Sunyaev R., 1988, Sov. Astron. Lett., 14, 390
 Makishima K., Mihara T., Ishida M., et al., 1990, ApJ, 365, L59
 Meszaros P., 1992, High-energy radiation from magnetized neutron stars (univ. of Chicago Press)
 Meszaros P., Nagel W., 1985, ApJ, 299, 138
 Mihara T., Makishima K., Ohashi T. et al., 1990, Nature, 346, 250
 Mihara T., Makishima K., Nagase F. 1998, Adv. Space Res., 22, 987
 Mihara T., Terada Y., Nakajima M. et al., 2007, Progress of Theoretical Physics, 169, 191
 Negueruela I., Roche P., Fabregat J. et al., 1999, MNRAS, 307, 695
 Pavlov G., Shibanov Yu., Silant’ev N., Nagel W., 1985, ApJ, 291, 170
 Staubert R., Kendziorra E., Pietsch W. et al., 1980, ApJ., 239, 1010
 Staubert R., 2003, Chin. J. Astron. Astrophys., Vol 3, Suppl., 270

- Staubert R., Shakura N.I., Postnov K. et al., 2007, *A&A*, 465, L25
- Stella L., White N.E., Davelaar J., et al., 1985, *ApJ*, 288, L45
- Swank J., Remillard R., Smith E., 2004, *Astron. Telegram*, 349, 1
- Trümper J., Pietsch W., Reppin C. et al., 1977, *Annals of the New York Academy of Sciences*, 302, 538
- Tsygankov S.S., Lutovinov A.A., Churazov E.M., Sunyaev R.A., 2007, *Astron. Lett.*, 33, 368
- Tsygankov S.S., Lutovinov A.A., Churazov E.M., Sunyaev R.A., 2006, *MNRAS*, 371, 19
- White N., Swank J., Holt S., 1983. *ApJ*, 270, 711
- Zheleznyakov V.V. and Serber A.V., 1993. *Astron. Rep.*, 37, 507